ACS APPLIED MATERIALS & INTERFACES

Research Article

www.acsami.org

Superhydrophobic Colloidally Textured Polythiophene Film as Superior Anticorrosion Coating

Al Christopher C. de Leon,[†] Roderick B. Pernites,[‡] and Rigoberto C. Advincula*[,†,§]

[†]Department of Chemistry and Department of Chemical and Biomolecular Engineering, University of Houston, Houston, Texas 77204-5003, United States

[‡]Department of Chemical and Biomolecular Engineering, Rice University, MS 362, 6100 Main Street, Houston, Texas 77005, United States

[§]Department of Macromolecular Science and Engineering, Case Western Reserve University, Cleveland, Ohio 44106, United States

Supporting Information

ABSTRACT: In this paper, we demonstrated for the first time the use of electrodeposited superhydrophobic conducting polythiophene coating to effectively protect the underlying steel substrate from corrosion attack: by first preventing water from being absorbed onto the coating, thus preventing the corrosive chemicals and corrosion products from diffusing through the coating, and second by causing an anodic shift in the corrosion potential as it galvanically couples to the metal substrate. Standard electrochemical measurements revealed the steel coated with antiwetting nanostructured polythiophene film, which was immersed in chloride solution of different pH and temperature for up to 7 days, is very well protected from corrosion evidenced by protection efficiency of greater than 95%. Fabrication of the dual properties superhydrophobic anticorrosion nanostructured conducting polymer coating follows a two-step coating procedure that is very simple and can be used to coat any metallic surface.

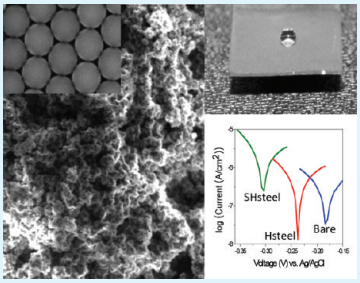

KEYWORDS: *superhydrophobic, anticorrosion, nanoparticles, conducting polymer, electrodeposition*

INTRODUCTION

Termed as the reverse metallurgy, corrosion is a very thermodynamically favorable process − converting a metal from its higher energy pure form to its lower energy oxide form.[1−10] Corrosion poses a serious economic and industrial threat, as well as, potential danger to humans. Unfortunately, corrosion cannot be prevented, and thus corrosion control strategies focus on slowing the kinetics and/or altering its mechanism. Corrosion control strategies can involve cathodic protection,[1,2] use of protective coating,[3−5] use of corrosion inhibitors,[6,7] or any combination thereof.[8−10] Another approach incorporates chromium into the alloy, as in the case for stainless steel.[11,12] Stainless steel is a low carbon steel with at least 10.5% chromium. When exposed to a corrosive environment, the chromium reacts with the oxygen to form a passive layer that is too thin (~130 Å) to be visible and causes the metal surface to remain lustrous. The chromium oxide layer significantly slows down the corrosion rate; however, halogen ions (e.g., chloride ions) can penetrate through and can cause breakdown of the passive layer.[13,14] Halogens can cause crevice and pitting corrosions that grow perpendicularly to the surface being attacked. For applications that involve substances capable of donating halogen ions, stainless steel is not recommended unless it has a protective coating. Various inorganic materials such as chromate,[15] organic materials such as conducting polymers,[5,16,17] and organic−inorganic composites such as organo-silicate composites[18] have been used as protective coatings. Currently, the most effective treatment is chromate-containing coatings; however, because of its high toxicity, which is threatening to human health and the environment, its use will eventually be banned.[19,20] One good alternative to chromate-containing coating could be a superhydrophobic coating made up of a conducting polymer.

Considerable interest has now been given to the use of superhydrophobic films as protective coatings.[21−23] Briefly, superhydrophobic coatings are characterized by a water contact angle of at least 150° and are known to be very resistant to water absorption.[24] This antiwetting property is relevant to its prevention from corrosion attack. For instance, water serves as a medium for the diffusion of corrosive chemicals and corrosion products; therefore, inhibiting water from being absorbed by the coating, which prevents these chemicals from reaching the metal-coating interface. This method is believed to provide superior corrosion protection compared to other methods. Fabrication of the superhydrophobic coating requires two things: (1) the material for coating should have low surface energy, and (2) it has roughness of micro- and nanoscale. Several materials have been used in fabricating super-hydrophobic coatings,[21,22] but those made from conducting polymers offer more than barrier protection against corrosion.

Received: March 22, 2012
Accepted: June 4, 2012
Published: June 4, 2012

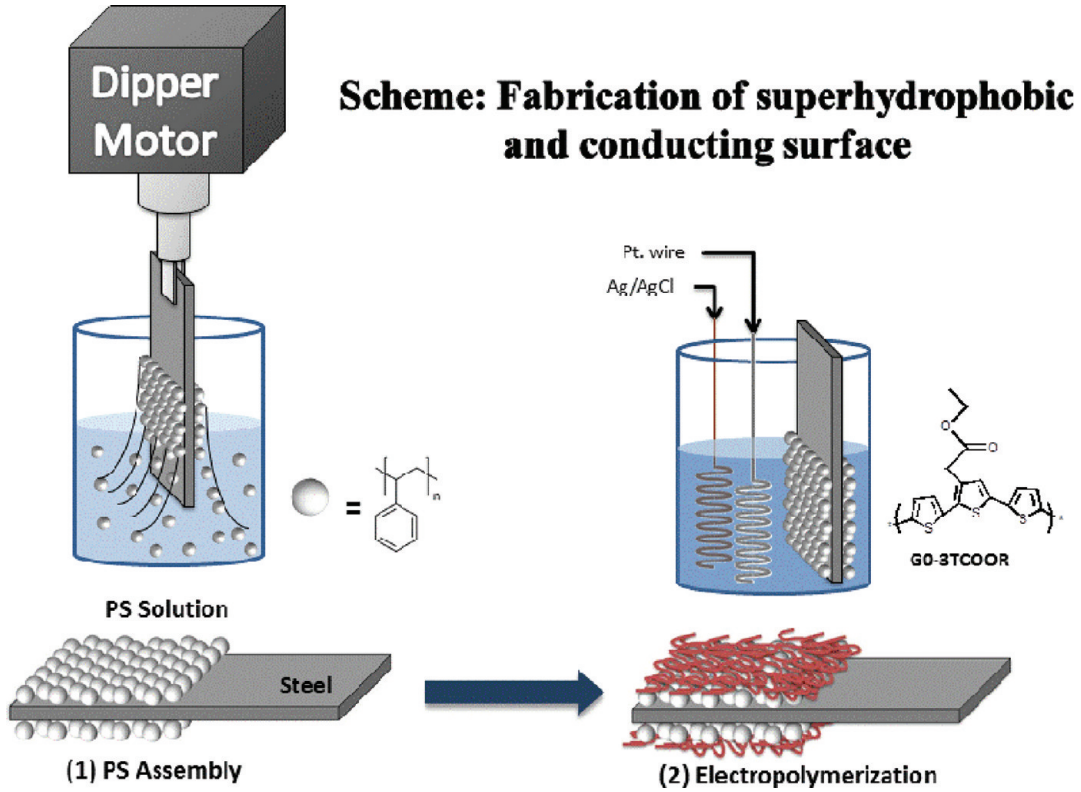

Figure 1. Fabrication scheme of the dual superhydrophobic and anticorrosion poly(G0−3T COOR) film by (1) polystyrene nanoparticle deposition, and (2) electropolymerization of G0−3T COOR.

Conducting polymers consist of π-conjugated chains, which contain highly delocalized electrons capable of transferring charges.[5] Conducting polymers protect the metal surface not only by acting as a barrier but also by causing anodic shift in the corrosion potential as they galvanically couple to the metal.[25] The shift causes the passivation and anodic protection of the metal substrate.[26] Also, it has been observed that conducting polymers can reduce the rate of corrosion even after the coating has been breached and metal surface has been exposed to the environment.[27] Anticorrosion properties of conducting polymer such as polyaniline, polypyrrole, and poly(vinylcarbazole) on steel substrates have been extensively studied.[3−5] In terms of film-forming properties, polythiophene, which is not commonly studied and applied for anticorrosion purposes, stands out among the others because of its capability to form a highly conjugated network.[28] Also, depending on the side-chain group, it can have very low surface energy, which is necessary for making a superhydrophobic surface. Our group has done several studies on the use of conducting polymers in various applications such as fabrication of superhydrophobic surfaces,[28−30] and coatings for corrosion protection[5] to list a few.

This work reports the outstanding capability of a superhydrophobic polythiophene coating in protecting stainless steel from corrosion due to chloride attack. This can be achieved with a very simple two-step process. First is the vertical deposition of polystyrene (PS) nanoparticles, which provides the microscale roughness necessary to make the surface superhydrophobic. Also, the polystyrene layer acts as another barrier to water, corrosive chemicals, and corrosion product diffusion. Second is the electropolymerization or electrodeposition of the terthiophene-derivative monomer, which provides the low surface energy coating, additional nanometer-scale roughness and porosity, and anodic protection of the underlying stainless steel substrate. Details are discussed in the Methods section. One major advantage of this facile fabrication approach is that the two-step coating procedure is nonspecific to stainless steel only but can be theoretically used to any metal surface like copper, aluminum, etc. In this study, the corrosion resistance of the modified stainless steel samples was measured by standard electrochemical measurements when they were immersed into a 3.5 M NaCl solution of different pH levels (i.e., pH 1, 7, and 14) and also at an elevated temperature. The results of the electrochemical measurements were then utilized to quantify the corrosion protection efficiency and qualitatively estimate the extent of coating degradation. Also, the anticorrosion performance of the superhydrophobic coating was compared to the stainless steel coated with just the electrodeposited polythiophene and bare stainless steel as the controls.

RESULTS AND DISCUSSION

To fabricate the superhydrophobic film-coated stainless steel (SHsteel), we first vertically deposited polystyrene nanoparticles onto the stainless steel substrate using Langmuir−Blodgett (LB)-like technique. This step was followed by the electrodeposition of the conducting polymer using the terthiophene monomer with the ester moiety side chain ethyl 2-(2,5-di(thiophen-2-yl)thiophen-3-yl)acetate or abbreviated as (G0−3T COOR) as shown in Figure 1. On the other hand, the fabrication of the hydrophobic film-coated stainless steel (Hsteel) involves only the electrodeposition of the polythiophene onto the surface of the bare stainless steel.

Electropolymerization was monitored by cyclic voltammetry as shown in Figure 2. As the polymerization proceeds, the

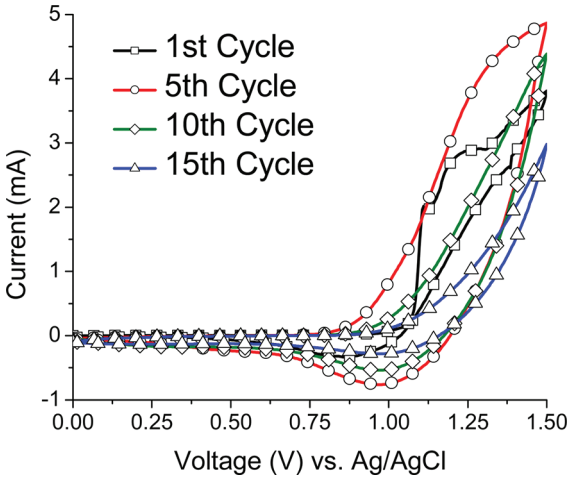

Figure 2. Cyclic voltammogram for electrodeposition of G0−3T COOR onto PS-coated stainless steel substrate.

current increases with the number of cycle until the fifth cycle. Consistent with previous observations,[31] the oxidation onset for terthiophene monomer is at 0.85 V. During the anodic scan of the first cycle, terthiophene radical cations are produced, which upon the cathodic scan, combine with other terthiophene radical cations to form dimers. Subsequent cycles produce more radical cations that combine to form a longer, more conjugated polythiophene. The polymer either grows from the monomer initially adsorbed on the surface or is deposited on the stainless steel after their molecular weight becomes so high that they precipitate out of the solution.[32] Two peaks can be seen at first cycle and are combined in later cycles. This has been interpreted as being a two-electron oxidation process that is later transitioned to be a single-electron process.[33] Starting in the sixth cycle, the current starts to decrease with increasing cycle number brought about by the increase in electrical resistance of the film as its thickness increases. After electropolymerization, the resulting film was washed with acetonitrile. The monomer-free scan shows the same redox couple during electropolymerization, which is evidence of a successful electrodeposition of the conjugated polymer onto the PS-coated surface (see the Supporting Information, Figure S1).

The elemental composition of the electropolymerized film on the surface was determined by X-ray photoelectron spectroscopy (XPS). The survey scan (see the Supporting Information, Figure S2) shows the expected elemental peaks of the polythiophene namely carbon (C), oxygen (O), and sulfur (S) atoms. Furthermore, the high- resolution XPS scan determines the presence of the S 2p peak on the surface between 162 and 165 eV (see the Supporting Information, Figure S2 inset), which validates the presence of the sulfur atom of the thiophene ring, which is the signature peak for polythiophenes.[34] Attenuated total reflectance infrared (ATR IR) spectroscopy was utilized to further confirm the deposition of poly(G0−3T COOR). The ATR IR spectra (see the Supporting Information, Figure S3) reveals the characteristic peaks of poly(G0−3T COOR): C−O stretch (1275−1391 cm^{-1}), C═C stretch (1660 cm^{-1}), C═O stretch (1729 cm^{-1}), linear C−H stretch (2847−3028 cm^{-1}), and aromatic C−H stretch (3035−3161 cm^{-1}).[28] Also, the UV spectrum (see the Supporting Information, Figure S4) of the same film fabricated onto transparent ITO substrate presents the characteristic $\pi \rightarrow$ π^* transition of the poly(G0−3T COOR) film at maximum absorption peak (λ_{max}) of 440 nm.[31]

Surface wettability of various substrates were characterized by static water contact angle measurements using ∼1−2 μL of water. Figure 3 depicts the hydrophilicity of bare stainless steel

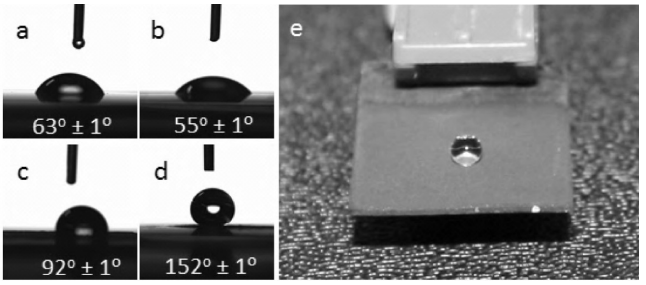

Figure 3. Static water contact angle of (a) bare, (b) PS-coated, (c) Hsteel, and (d) SHsteel. (e) Photograph image of water droplet on the SHsteel.

with a contact angle of 63°. The water layer film can easily form at the surface of bare stainless steel which makes the surface of the metal vulnerable to corrosion attack. Deposition of a monolayer of PS nanoparticles onto the surface of stainless steel nor electropolymerization of G0−3T COOR on top of bare stainless steel (without PS nanoparticles) do not provide resistance to formation of a water layer, as evidenced by very low contact angle of 55° ± 1° and 92° ± 1° (which is characteristic of hydrophobic film), respectively. Coating the stainless steel with a hydrophobic material is expected to marginally prevent the absorption of water through the coating and thus decrease to some extent the rate of diffusion of corrosive chemicals to the metal−polymer interface. The contact angle of a hydrophobic film can be significantly increased by making the surface relatively rough as implied by the Wenzel Model.[35] The superhydrophobic property depends strongly on the surface roughness, and surface energy.[36] For this system, surface roughness was controlled by using the PS nanoparticles of various diameters and by varying the rate of electrodeposition, which is related to the thickness of the deposited polymer film (see the Supporting Information, Table S1). In principle, the nanoparticles provide microscale roughness while the deposited conducting polymer provides the nanoscale roughness, porosity, and low surface energy. To fabricate a superhydrophobic film, the nanoparticle size and polymer thickness should be optimized. A polymer coating that is too thin and produced via a very high scan rate can result in incomplete coverage of the PS nanoparticle monolayer and drastically lowers the contact angle. Although thick polymer coatings (very low scan rate) can prevent exposure of PS nanoparticle, it is still unfavorable because it can compromise the film stability (attachment to the surface) and it can also render the microscale roughness provided by the nanoparticles useless. Optimization experiments have revealed that superhydrophobic film can be fabricated by using 500 nm PS nanoparticles and via 5 mV/s CV scan rate.

To examine the influence of surface morphology on the superhydrophobic nature of the resulting film, Scanning Electron Microscope (SEM) is utilized to capture the surface images at high magnification. Figure 4a displays the SEM images of the SHsteel and underlying PS nanoparticle monolayer (inset). As observed in Figure 4a, a monolayer of PS nanoparticles induces the electropolymerization of G0−3T

dx.doi.org/10.1021/am300513e | ACS Appl. Mater. Interfaces 2012, 4, 3169−3176

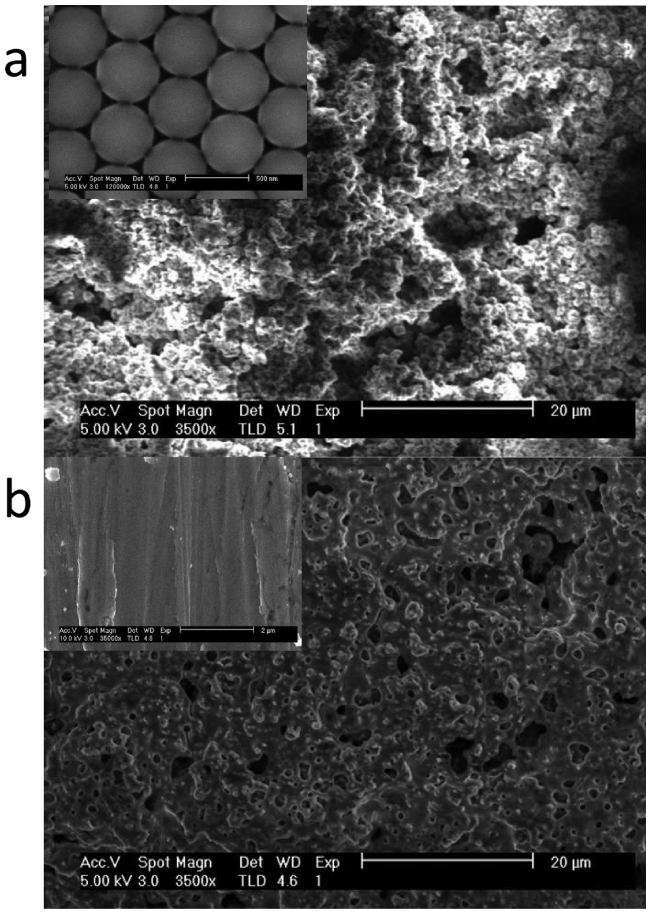

Figure 4. (a) SEM Image of SHsteel with inset of SEM image of PS nanoparticles layered onto the steel before CV-electrodeposition, (b) SEM Image of Hsteel with inset of SEM image of bare stainless steel.

COOR with very rough surface topography. This topography with hierarchical roughness and high porosity, coupled with very low surface energy of the coating material, causes very high water contact angle (or strong repellence to water adhesion). Air is believed to be entrapped in the nanopores which functions as another diffusion barrier to water due to the minimal contact between the water droplet and the surface. Figure 4b, on the other hand, displays the surface topography of the hydrophobic film and the underlying polished stainless steel surface (inset). In contrast to the morphology of SHsteel, Hsteel surface is relatively smooth and has few sites that can trap air. The perceptible disparity in surface morphology explains the significant difference between the water contact angles for SHsteel and Hsteel substrates.

It has been established that for a coating to be effective in preventing corrosion of the underlying substrate, it has to be able to prevent the diffusion of water through it.[21] Absorption of water by the coating can form a diffusion pathway for oxygen and chloride ions.[22] Continuous supply of oxygen ensures the cathodic reaction proceeds.[1] Diffusion of chloride ions, on the other hand, causes crevices and pits growing perpendicularly to the surface.[11] It is therefore reasonable to assume that increasing the water repellant property of the coating increases its ability to protect the underlying substrate from corroding.

To quantitatively measure the corrosion protection efficiency of the coatings, a potentiodynamic polarization experiment was done. Bare stainless steel, Hsteel, and SHsteel were immersed in 3.5 M NaCl solution. The samples were immersed for 1 day before doing any measurements to make sure that the system is in steady-state. Corrosion performance of the samples can be inferred by analysis of the corrosion potential (E_{corr}) and corrosion current (I_{corr}). These parameters are extracted from the potentiodynamic polarization curves via a computer routine by specifying the cathodic and anodic branches and using nonlinear least-squares fitting method of Levenberg/Marquardt.[37] This procedure is a significant improvement over the traditional Tafel extrapolation method.[38] Protection efficiency was calculated by using the following formula (eq 1)

$$PE = \frac{I_{corr,bare} - I_{corr,coated}}{I_{corr,bare}} \times 100\% \quad (1)$$

where $I_{corr,bare}$ and $I_{corr,coated}$ are the corrosion current density for uncoated and coated stainless steels, respectively.

The polarization curves and the calculated Tafel parameters for the three samples after immersion in 3.5 M NaCl solution are presented in Figure 5 (pH 7) and summarized in Table 1 (under pH 7), respectively. E_{corr} for bare stainless steel and Hsteel were determined to be −307 mV and −237 mV, respectively. E_{corr} is a measure of tendency of the sample to corrode and protection efficiency of coating; as the value of E_{corr} becomes more positive, the efficiency of protection increases.[39] The positive shift in E_{corr} suggests the efficient protection of stainless steel by the conducting polymer coating. Also, the measured corrosion current for Hsteel (i.e., 0.271 μA cm^{-2}) is lower than the corrosion current for bare stainless steel (i.e., 1.600 μA cm^{-2}). This can be attributed to the ability of the conducting polymer to (1) act as a barrier and decrease the amount of water, oxygen, and chloride ions at the metal−polymer interface, and (2) form protective passive layer on the stainless steel surface because of its redox catalytic properties.[40]

Corrosion protection can be significantly improved by making the conducting polymer film superhydrophobic. Compared to Hsteel, E_{corr} of SHsteel is more positive (−183 mV) and its I_{corr} is also lower (0.005 μA cm^{-2}). The enhancement of protection is caused by the effective prevention of water from diffusing through the nanostructured coating. The determined morphology of the superhydrophobic surface shows hierarchical roughness and high porosity that is believed to entrap air, and thus minimizing contact between water and the surface. Because of the very low diffusion coefficient of water though air, it takes a lot of time for water to diffuse through air layer.

The outstanding corrosion protection capability of SHsteel was further investigated by measuring the E_{corr} and I_{corr} after immersion in 3.5 M NaCl solution for 7 days. Extended immersion of bare stainless steel causes the E_{corr} to shift to −441 mV and I_{corr} to increase to 2.820 μA cm^{-2}. This is equivalent to 76.3% increase in corrosion rate. As for the Hsteel, E_{corr} and I_{corr} changed to −289 mV and 0.579 μA cm^{-2}. This is equivalent to drop of protection efficiency from 83 to 63.8%. In contrast, SHsteel showed minimal decrease in performance as evidenced by the calculated E_{corr} of −196 mV and I_{corr} of 0.013 μA cm^{-2}. The change is equivalent to minimal efficiency drop from 96.2 to 93.1%. It can be seen that even after 7 days of immersion, the SHsteel performs better than Hsteel.

Moreover, the polarization curves for the three samples were measured at different pH (by adding HCl and NaOH) and at an elevated temperature to demonstrate the superior perform-

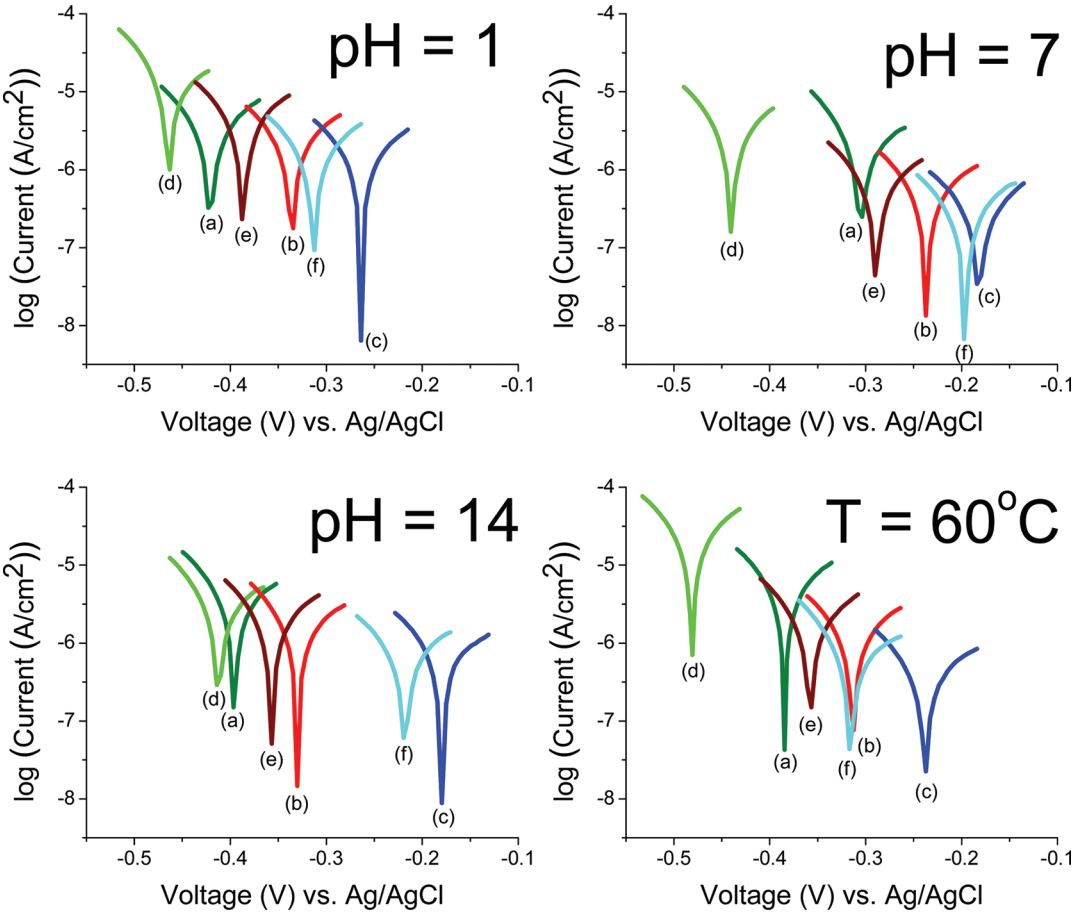

Figure 5. Potentiodynamic polarization scans of (a, d) bare stainless steel, (b, e) Hsteel, and (c, f) SHsteel measured after 1 day and 7 days of immersion, respectively, in 3.5 M NaCl solution of varying pH (kept at 25 °C) and at high temperature (60 °C, pH 7).

ance of SHsteel over Hsteel in different corrosive environment conditions. As shown in Table 1 (pH 1), addition of HCl increases the I_{corr} for bare stainless steel to 2.550 μA cm^{-2}. Addition of HCl exacerbates the corrosive attack to the passive layer of the chloride ions.[41] The protection efficiency for SHsteel is calculated to be 96.6%, which is much higher than the protection efficiency for Hsteel (72.5%). Even in acidic environments, water cannot diffuse through the superhydrophobic coating and the accelerating effect of hydrogen ions on corrosion is prevented. After 7 days of immersion, SHsteel showed a small change in protection efficiency, but note that it is still much higher than that for Hsteel.

Performance of SHsteel and Hsteel was also evaluated in a highly alkaline chloride environment. Although the alkaline environment actually helps protect the stainless steel by accelerating the formation of the passive layer, corrosion is still not fully prevented because of the chloride ions that destroy the passive layer.[42] After 1 day of immersion, results show that SHsteel has a protection efficiency of 96.2%, whereas the Hsteel has a protection efficiency of 81.3% only. Extended immersion for 7 days of both samples yields protection efficiencies of 93.1 and 66.4% for SHsteel and Hsteel, respectively.

Corrosion rate is known to significantly augment when increasing the temperature of the corrosive environment.[43] To see how SHsteel and Hsteel perform under this condition, the samples were immersed in a neutral 3.5 M NaCl solution and heated to 60 °C. After 1 day, polarization scans reveal that the SHsteel performs better than Hsteel with a protection efficiency of 95.8 vs 65.0%. After 7 days, the protection efficiency for SHsteel remained high at 93.9%, whereas protection efficiency for Hsteel dropped to 56.9%. These results exemplify the effect of preventing water from diffusing through the coating. The stainless steel surface is deprived of oxygen and thus the extent at which the cathodic reaction happens is very limited. Chloride ion concentration is also kept at minimum and thus the passive layer remains intact, and crevices and pitting corrosions are therefore prevented.

To better understand the superior performance of SHsteel, electrochemical impedance spectroscopy was employed. Impedance spectroscopy is a nondestructive method of determining several system parameters like the degree of coating degradation and coating capacitance and resistance, which are related to the extent of water and ion absorption, respectively.[44] Similarly, SHsteel and Hsteel were exposed to 3.5 M NaCl solution for 1 day and 7 days. The electrochemical behavior and film degradation were monitored by applying alternating current of 10 mV amplitude and of varying frequency from 100 kHz to 10 mHz.[45] The frequency is usually swept from higher frequency to lower frequency to minimize the perturbation of the sample.[44] The Bode plots obtained for SHsteel and Hsteel are shown in panels a and b in Figure 6, respectively, as function of immersion time. After 1 day of immersion, the Bode magnitude plot for Hsteel shows a very low overall impedance value of 1.8 kΩ cm^2 at low frequency end. SHsteel on the other hand shows overall

dx.doi.org/10.1021/am300513e | ACS Appl. Mater. Interfaces 2012, 4, 3169−3176

Table 1. Tafel Parameters for Coated and Uncoated Stainless Steels after Immersion in 3.5 M NaCl Solution of Varying pH and at High Temperature for 1 day and 7 days

	immersion period (days)	E_{corr} (mV) vs Ag/AgCl	I_{corr} (μA cm^{-2})	corrosion rate (mm/year)	protection efficiency (%)
pH 1					
bare stainless steel	1	−421	2.550	2.96×10^{-2}	
Hsteel	1	−336	0.699	8.12×10^{-3}	72.5
SHsteel	**1**	**−264**	**0.009**	$\mathbf{1.01 \times 10^{-3}}$	**96.6**
bare stainless steel	7	−464	6.900	8.01×10^{-2}	−170.8
Hsteel	7	−387	1.130	1.32×10^{-2}	55.5
SHsteel	**7**	**−313**	**0.322**	$\mathbf{3.74 \times 10^{-3}}$	**87.4**
pH 7					
bare stainless steel	1	−307	1.600	1.86×10^{-2}	
Hsteel	1	−237	0.271	3.15×10^{-3}	83.0
SHsteel	**1**	**−183**	**0.005**	$\mathbf{5.75 \times 10^{-4}}$	**96.9**
bare stainless steel	7	−441	2.820	3.27×10^{-2}	−76.3
Hsteel	7	−289	0.579	6.73×10^{-3}	63.8
SHsteel	**7**	**−196**	**0.008**	$\mathbf{9.82 \times 10^{-4}}$	**94.7**
pH 14					
bare stainless steel	1	−396	1.870	2.18×10^{-2}	
Hsteel	1	−330	0.351	4.07×10^{-3}	81.3
SHsteel	**1**	**−179**	**0.007**	$\mathbf{8.24 \times 10^{-4}}$	**96.2**
bare stainless steel	7	−412	4.620	5.36×10^{-2}	−146.3
Hsteel	7	−357	0.629	7.31×10^{-3}	66.4
SHsteel	**7**	**−218**	**0.013**	$\mathbf{1.50 \times 10^{-3}}$	**93.1**
T = 60 °C					
bare stainless steel	1	−385	3.32	3.85×10^{-2}	
Hsteel	1	−313	1.16	$1.35x\ 10^{-2}$	65.0
SHsteel	**1**	**−238**	**0.14**	$\mathbf{1.63 \times 10^{-3}}$	**95.8**
bare stainless steel	7	−481	11.7	1.36×10^{-1}	−252.7
Hsteel	7	−358	1.46	1.69×10^{-2}	56.0
SHsteel	**7**	**−315**	**0.20**	$\mathbf{2.36 \times 10^{-3}}$	**93.9**

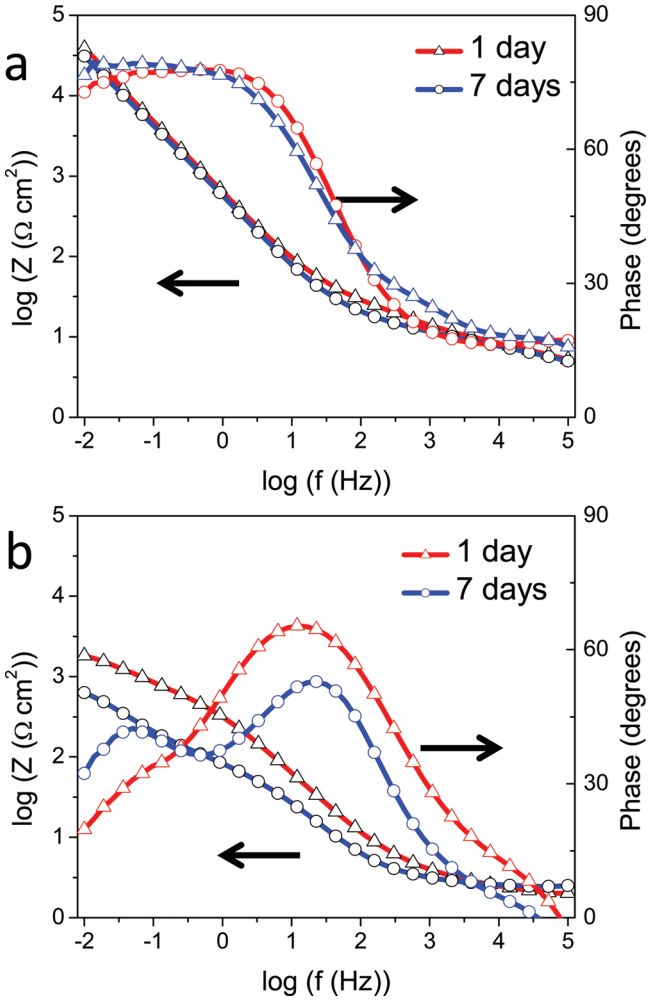

Figure 6. Bode plot of (a) SHsteel and (b) Hsteel immersed in 3.5 M NaCl solution for 1 day and 7 days.

impedance value of 39 kΩ cm^2, which is almost 22 times larger than that of Hsteel. Immersion of Hsteel for 7 days decreases the overall impedance to 0.6 kΩ cm^2 at low frequency. Low overall impedance value could be brought about by very high capacitance and/or very low resistance of the coating.[46,47] Large value of the capacitance has been related to the high extent at which water has penetrated the coating.[27] Also, the small resistance value has been related to (1) high extent of formation of ionically conducting path across the coating brought about by diffusion of electrolytes through the coating, and (2) increase in coating delamination area.[48] The overall impedance value for SHsteel remained high at 31 kΩ cm^2 after 7 days of immersion.

On the other hand, the phase angle is a very sensitive indicator of the polymer coating damage.[27] In particular, the presence and increase in breakpoint frequency (f_b), presence of minimum phase angle (θ_{min}) and its frequency (f_{min}) indicate increasing degree of delamination. After immersion of Hsteel for 1 day, Figure 6b shows evidence of delamination as indicated by the presence of f_b at 0.66 Hz and increase to 3.3 Hz after 7 days of immersion in 3.5 M NaCl solution. Also after 7 days, θ_{min} at 36.41° and f_{min} of 0.48 Hz appear in the Bode phase plot for Hsteel. As expected for SHsteel, such parameters cannot be seen which indicates that even after 7 days of immersion the coating remained intact. This result further proves the superiority of superhydrophobic coating in protecting the underlying metal substrate by preventing the water and electrolyte from diffusing through the coating and being resistant to delamination in the presence of a corrosive environment.

CONCLUSION

In this study, we have proven that superhydrophobic conducting polymer coating fabricated by simple two-step process has superior corrosion protection capability as compared to hydrophobic coating of the same polymer material after immersing in 3.5 M NaCl solutions of a wide pH value range and at elevated temperatures. The superior performance can be attributed to the high water repellency of the polymer coating combined with its capability to protect the substrate anodically. The ability of the coating to prevent the adhesion of water is important to its anticorrosion property as water serves as the medium for diffusion of aggressive chemicals and corrosion products, from being absorbed by the coating. Also, the nonspecificity of the coating procedure to stainless steel may prove advantageous in protecting other metallic substrates against corrosion.

EXPERIMENTAL SECTION

Materials and Substrate Preparation. *Stainless Steel Substrate Preparation.* Stainless steel foils (Alfa Aesar, Type 304) with composition Fe:Cr:Ni; 70:19:11 wt % were cut into 2 cm × 1.5 cm pieces. The stainless steel substrates were polished with increasing grades of emery papers (80, 400, 600, and 1200), sonicated in acetone for 15 min, and were dried under N_2 stream prior to use.

Polystyrene Nanoparticle Layer. One weight percent PS nanoparticle solution was prepared by mixing 500 nm PS latex microbeads (Polysciences, Inc.) with 34.7 mM sodium n-dodecyl sulfate (Sigma Aldrich) in Milli-Q water (18.2 MΩ cm resistivity). The resulting solution was sonicated for at least 30 min prior to use to ensure that the PS particles are well dispersed. The nanoparticles were deposited by procedure similar to what Grady and co-worker have reported earlier.[49] The stainless steel substrate was clipped vertically into the dipper and was dipped into the PS nanoparticle solution (Figure 1). The stainless steel substrate was vertically withdrawn by using the dipper motor at a lift-up rate of 0.1−0.3 mm/s. The resulting film was dried by suspending it for few minutes.

Electropolymerization of Terthiophene-Derivative Monomer. The monomer solution used in electropolymerization was prepared by mixing the monomer, ethyl 2-(2,5-di(thiophen-2-yl)thiophen-3-yl)acetate (G0−3T COOR), which was synthesized in our laboratory,[28] acetonitrile solvent (Sigma-Aldrich), and tetrabutylammonium hexafluorophosphate (Sigma Aldrich). Five mM of this solution was electropolymerized onto the PS nanoparticle-coated stainless steel substrate by cyclic voltammetry (CV) technique (Figure 1). The stainless steel substrate functioned as the working electrode, while Platinum (Pt) and Ag/AgCl wire as the counter and reference electrodes, respectively. Voltage was swept back and forth from 0 to 1.5 V for 15 cycles at a rate of 5 mV/s. The resulting film was washed with ACN and was dried under N_2 stream. For the monomer-free scan, the voltage was swept from 0 to 1.5 V for 10 cycles at a rate of 50 mV/s. The solution used contained acetonitrile and tetrabutylammonium hexafluorophosphate.

General Instrumentation. Electropolymerization and all electrochemical measurements were done using Autolab PGSTAT 12 Potentiostat (MetroOhm, Inc.). Potentiodynamic Polarization Scan was performed by scanning from −0.05 V to +0.05 V Ag/Ag^+ reference electrode (3.5 M NaCl) about the open circuit potential (OCP). Electrochemical impedance spectroscopy (EIS) was performed for seven frequency decades from 10 mHz to 100 kHz with an amplitude of 10 mV with respect to the OCP. For both measurements, platinum was used as counter electrode, Ag/Ag+ in 3.5 M NaCl was used as reference electrode, and the stainless steel substrates as the working electrodes.

Static water contact angle was measured by using a CAM 200 optical contact angle meter (KSV Instruments Ltd.). SEM analysis was done using FEI XL-30FEG SEM equipped with NPGS (Nanopattern Generation System). The ATR IR spectroscopy was done with Digilab FTS 7000 equipped with HgCdTe detector from 4000 to 600 cm^{-1}. The nominal spectral resolution is 4 cm^{-1}. The measurement was done in absorbance mode. XPS data (at takeoff angle of 45° from the surface) was recorded using a PHI 5700 X-ray Photoelectron Spectrometer with a monochromatic Al Kα X-ray source ($h\nu$ = 1486.7 eV) incident at 90° relative to the axis of hemispherical energy analyzer. UV−vis spectra were obtained by using an Agilent 8453 spectrometer.

ASSOCIATED CONTENT

Supporting Information

Additional figures (PDF). This material is available free of charge via the Internet at http://pubs.acs.org.

AUTHOR INFORMATION

Corresponding Author

*E-mail: radvincula@uh.edu. Phone: +1 713 743 1755.

Notes

The authors declare no competing financial interest.

REFERENCES

(1) Shen, G. X.; Chen, Y. C.; Lin, C. J. *Thin Solid Films* **2005**, *489*, 130−136.
(2) Yun, H.; Li, J.; Chen, H. B.; Lin, C. J. *Electrochim. Acta* **2007**, *52*, 6679−6685.
(3) Wessling, B. *Adv. Mater.* **1994**, *6*, 226−228.
(4) Kilmartin, P. A.; Trie, L.; Wright, G. A. *Synth. Met.* **2002**, *131*, 99−109.
(5) Frau, A.; Pernites, R. B.; Advincula, R. C. *Ind. Eng. Chem. Res.* **2010**, *49* (20), 9789−9797.
(6) Söylev, T. A.; Richardson, G. M. *Constr. Build. Mater.* **2008**, *22*, 609−622.
(7) Quraishi, M. A.; Rawat, J. *Mater. Chem. Phys.* **2002**, *73*, 118−122.
(8) Kendig, M.; Hon, M. *Prog. Org. Coat.* **2003**, *7*, 183−189.
(9) Suryanarayana, C.; Rao, K. C.; Kumar, D. *Prog. Org. Coat.* **2008**, *63*, 72−78.
(10) Kumar, A.; Stephenson, L. D.; Murray, J. N. *Prog. Org. Coat.* **2006**, *55*, 244−253.
(11) Streicher, M. A. *J. Electrochem. Soc.* **1956**, *103* (7), 375−390.
(12) Saidman, S. B.; Gonzalez, M. B. *Corros. Sci.* **2011**, *53*, 276−282.
(13) Sherif, E. M.; Potgieter, J. H.; Comins, J. D.; Cornish, L.; Olumbambi, P. A.; Machio, C. N. *Corros. Sci.* **2009**, *51* (6), 1364−1371.
(14) Martinez, C.; Sancy, M.; Zagal, J. H.; Rabagliati, F. M.; Tribollet, B.; Torres, H.; Pavez, J.; Monsalve, A.; Paez, A. *J Solid State Elctrochem* **2009**, *13*, 1327−1337.
(15) Kendig, M. W.; Davenport, A. J.; Isaacs, H. S. *Corros. Sci.* **1993**, *34* (1), 41−49.
(16) Carrasco, P. M.; Cortazar, M.; Ochoteco, E.; Calahorra, E.; Pomposo, J. A. *Surf. Interface Anal.* **2007**, *39*, 26−32.
(17) Yoon, H.; Chang, M.; Jang, J. *Adv. Funct. Mater.* **2007**, *17*, 431−436.
(18) Roussi, E.; Tsetsekou, A.; Tsiourvas, D.; Karantonis, A. *Surf. Coat. Technol.* **2011**, *205*, 3235−3244.
(19) Balaraju, J. N.; Rajam, K. S. *Int. J. Electrochem. Sci.* **2007**, *2*, 747−761.
(20) Hamid, Z. A. *Surf. Coat. Technol.* **2009**, *203*, 3442−3449.
(21) Weng, C. J.; Chang, C. H.; Peng, C. W.; Chen, S. W.; Yeh, J. M.; Hsu, C. L.; Wei, Y. *Chem. Mater.* **2011**, *23*, 2075−2083.
(22) Zhang, F.; Chen, S.; Dong, L.; Lei, Y.; Liu, T.; Yin, Y. *Appl. Surf. Sci.* **2011**, *257*, 2587−2591.
(23) Rao, A. V.; Latthe, S.; Mahadik, S.; Kappenstein, C. *Appl. Surf. Sci.* **2011**, *257*, 5772−5776.
(24) Hill, R.; Ma, M. *Curr. Opin. Colloid Interface Sci.* **2006**, *11*, 193−202.
(25) Tallman, D. E.; Spinks, G.; Dominis, A.; Wallace, G. C. *J Solid State Electrochem* **2002**, *6*, 73−100.
(26) Grgur, B. N.; Krstajic, N. V.; Vojnovic, M. V.; Lacnjevac, C.; Gajic-Krstajic, Lj. *Prog. Org. Coat.* **1998**, *33*, 1−6.
(27) Reinhard, G.; Rammelt, U. *Prog. Org. Coat.* **1992**, *21*, 205−226.
(28) Pernites, R.; Ponnapati, R.; Advincula, R. *Adv. Mater.* **2011**, *23*, 3207−3213.

(29) Pernites, R.; Santos, C.; Maldonado, M.; Ponnapati, R.; Rodrigues, D.; Advincula, R. *Chem. Mater.* **2011**.
(30) Pernites, R.; Ponnapati, R.; Advincula, R. *Adv. Mater.* **2011**, *23*, 3207−3213.
(31) Taranekar, P.; Fulghum, T.; Baba, A.; Patton, D.; Advincula, R. *Langmuir* **2007**, *23*, 908−917.
(32) Ludwigs, S.; Frontana-Uribe, B. A.; Heinze, J. *Chem. Rev.* **2010**, *110*, 4724−2771.
(33) Apodaca, D.; Pernites, R.; Ponnapati, R.; Del Mundo, F.; Advincula, R. *ACS Appl. Mater. Interfaces* **2011**, *3* (2), 191−203.
(34) Pernites, R.; Ponnapati, R.; Advincula, R. *Macromolecules* **2010**, *43* (23), 9724−9735.
(35) Wenzel, R. N. *Ind. Eng. Chem. Res.* **1936**, *28*, 988−994.
(36) Efimenko, K.; Genzer, J. *Biofouling* **2006**, *22*, 339−360.
(37) Balasubramaniam, R.; Bhardwaj, M. *Int. J. Hydrogen Energy* **2008**, *33*, 248−251.
(38) Stern, M. *J. Electrochem. Soc.* **1955**, *102*, 609−616.
(39) Gomes, E. C.; Oliviera, M. A. S. *Surf. Coat. Technol.* **2011**, *250*, 2857−2864.
(40) Delimi, A.; et al. *Surf. Coat. Technol.* **2011**, *250*, 4011−4017.
(41) Bhandari, H.; Srivastav, R.; Choudhary, V.; Dhawan, S. K. *Thin Solid Films* **2010**, *519*, 1031−1039.
(42) Cabrera-Sierra, R.; Miranda-Hernandez, M.; Sosa, E.; Oropeza, T.; Gonzalez.. *Corros. Sci.* **2001**, *43*, 2305−2324.
(43) Popova, A.; Sokolova, E.; Raicheva, S.; Christov, M. *Corros. Sci.* **2003**, *45*, 33−58.
(44) Thierry, D.; Amirudin, A. *Prog. Org. Coat.* **1995**, *26*, 1−28.
(45) Ates, M. *Prog. Org. Coat.* **2011**, *71*, 1−10.
(46) Kannan, M. B.; Gomes, D.; Dietzel, W.; Abetz, V. *Surf. Coat. Technol.* **2008**, *202*, 4598−4601.
(47) Hamdy, A; El-Shenawy; El-Bitar, T. *Int. J. Electrochem. Sci.* **2006**, *1*, 171−180.
(48) Mansfeld, F. *J. Appl. Electrochem.* **1995**, *25*, 187−202.
(49) Marquez, M.; Grady, B. P. *Langmuir* **2004**, *20*, 10998−11004.